Electronic Supplementary Material (ESI) for Journal of Materials Chemistry A.

Support Information

Panchromatic ternary/quaternary polymer/fullerene BHJ solar cells, based on novel silicon naphthalocyanine and silicon phthalocyanine dye sensitizers

Lili Ke[a*], Nicola Gasparini[a] , Jie Min[a], Hong Zhang[a], Matthias Adam[b], Stefanie Rechberger[c], Karen Forberich[a], Chaohong Zhang[a], Erdmann Spiecker[c], Rik R. Tykwinski[b], Christoph J. Brabec[a, d], Tayebeh Ameri[a*]

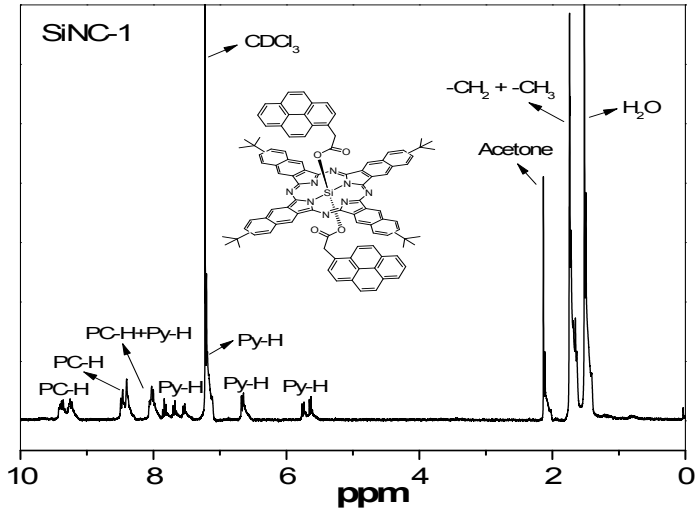

Fig. S1 ^{1}H NMR spectrum for **SiNC-1**. PC-H indicates those protons which are located in phthalocyanine ring, and Py-H those are located in pyrene rings. H_2O is from the test solvent $CDCl_3$, and the proton of acetone is because that the final compound is not sufficiently dry.

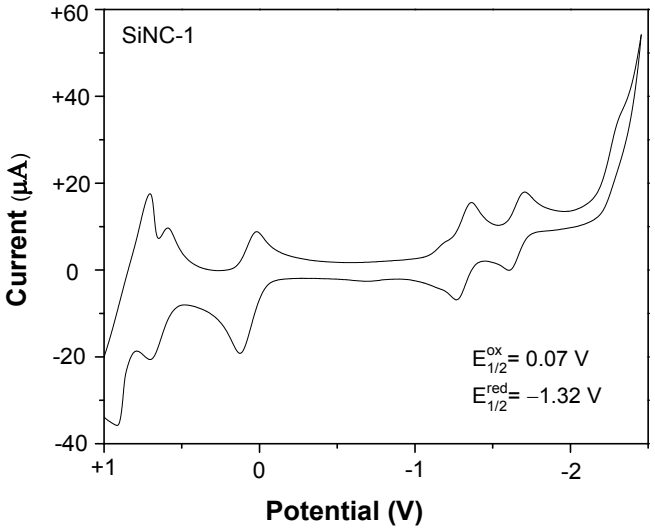

Fig. S2 Cyclic voltammagram of **SiNC-1**. The potentials are measured vs F_C/F_C^+, using Ag/AgCl as reference electrode. Ferrocene was measured separately.

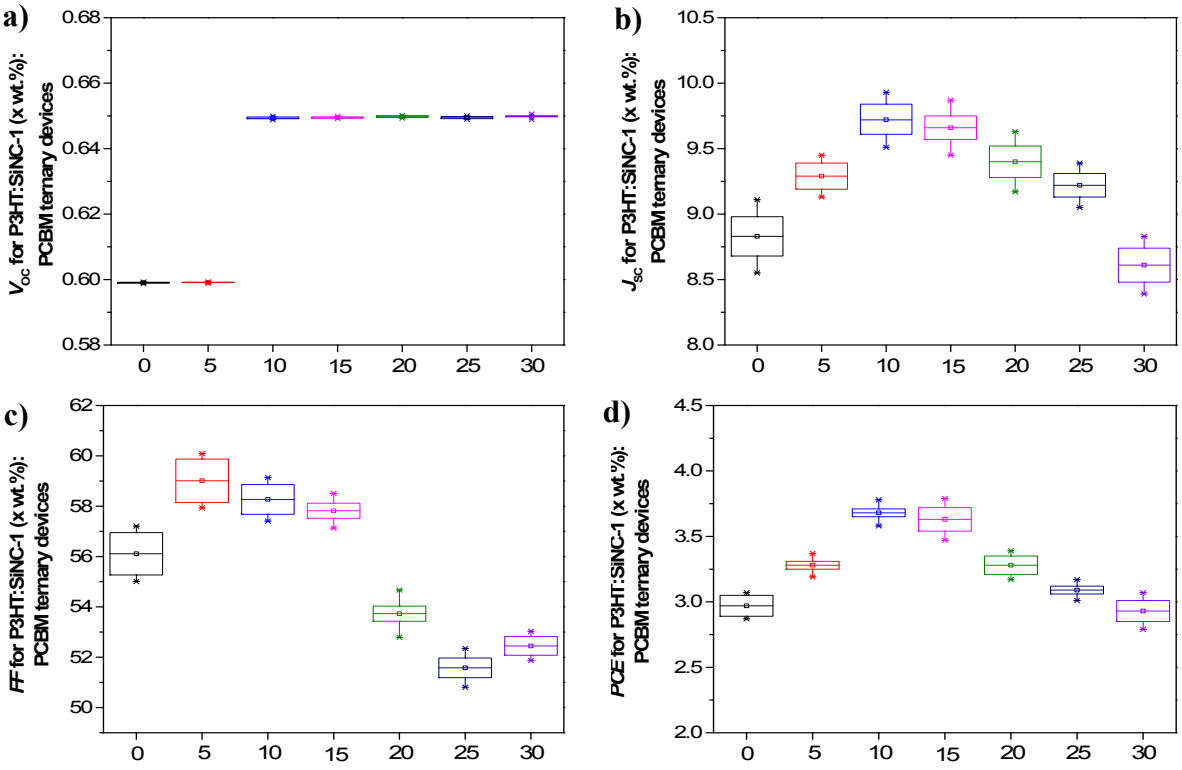

Fig. S3 Chart-box presentation of the a) V_{OC}, b) J_{SC}, c) FF and d) PCE values recorded for over 10 P3HT:**SiNC-1**:PCBM ternary blend solar cells versus **SiNC-1** contents.

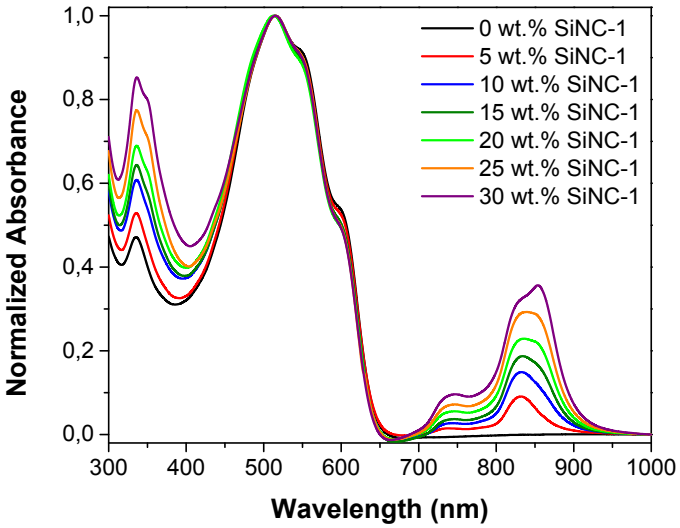

Fig. S4 Normalized absorption spectra of P3HT:**SiNC-1**:PCBM ternary films with increasing **SiNC-1** contents.

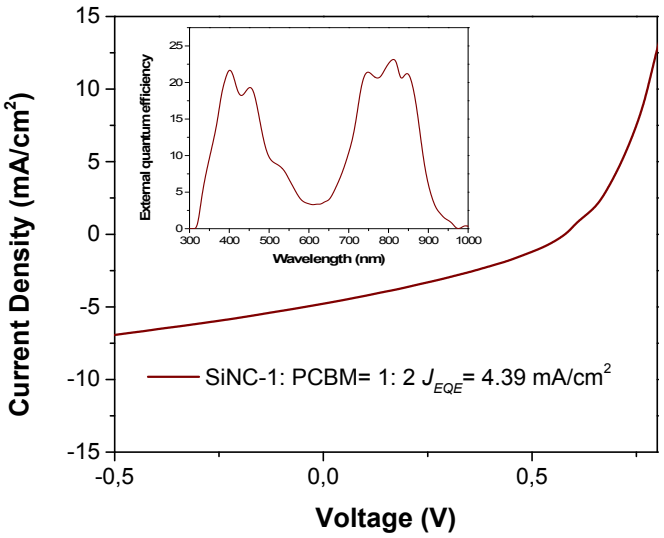

Fig. S5 The *J–V* curves and EQE spectra (inside figure) of **SiNC-1**:PCBM binary device.

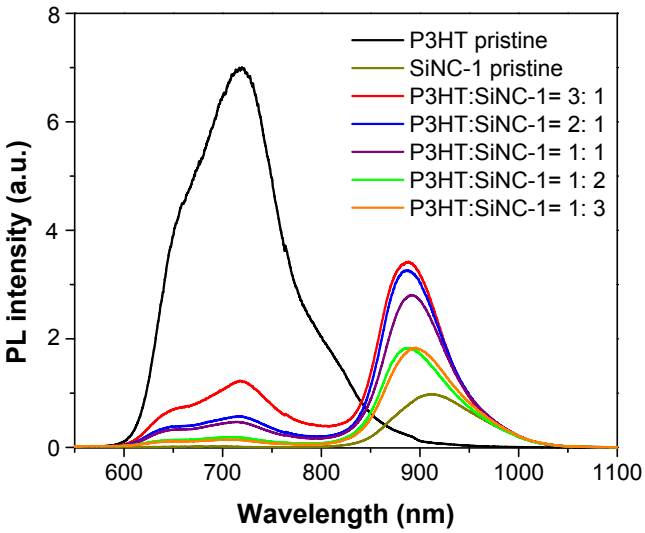

Fig. S6 Photoluminescence spectra of pristine P3HT and **SiNC-1**, P3HT:**SiNC-1** based binary films with different ratios.

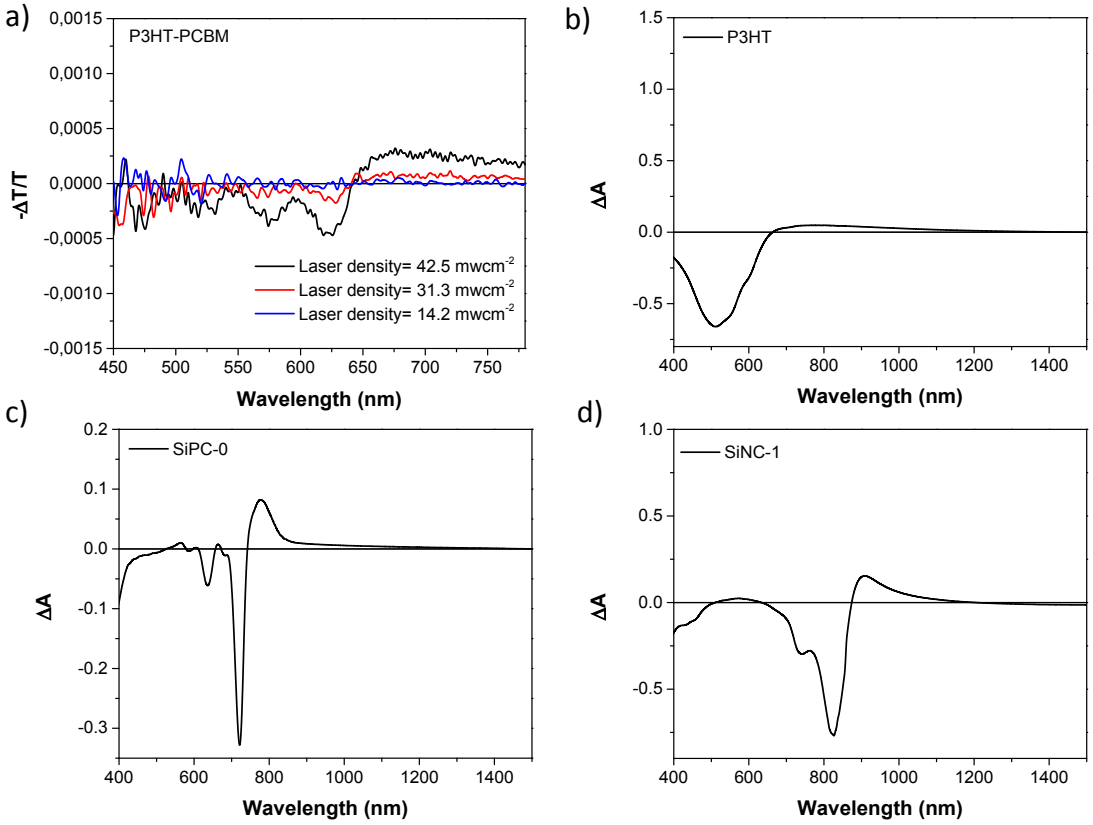

Fig. S7 a) PIA spectra recorded at 6.8 mw cm^{-2} light density at different laser intensity; The differential absorption spectrum of b) P3HT, c) **SiPC-0,** and d) **SiNC-1** which is obtained as the absorption difference between the doped and undoped spectra (doping method: mixing with iodine and coating by doctor blading).

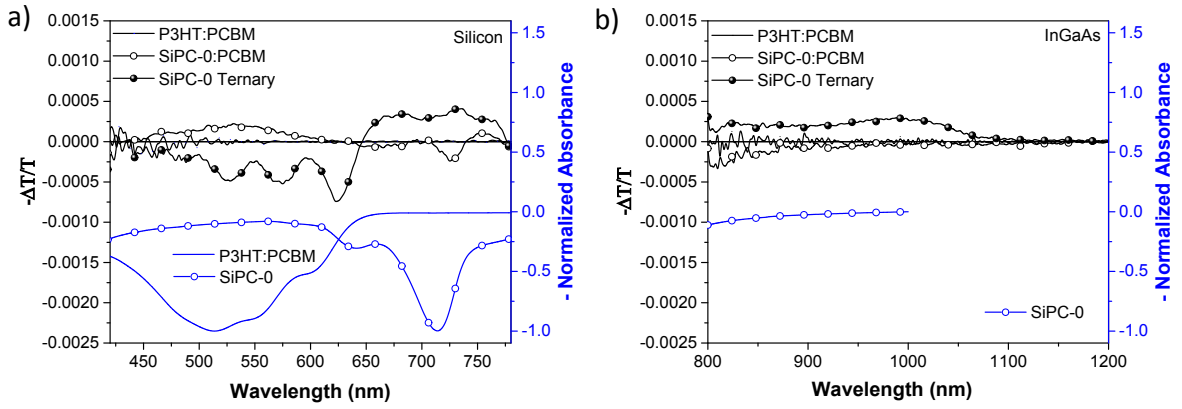

Fig. S8 PIA spectra recorded at 6.8 mw cm^{-2} light intensity and 14.2 mw cm^{-2} laser intensity of P3HT:PCBM, **SiPC-0**:PCBM, and **SiPC-0** based ternary films measured by a) silicon and b) InGaAs detectors. The normalized absorption spectra of the P3HT:PCBM and **SiPC-0** films

are presented on the same graphs for a direct comparison of the peak futures.

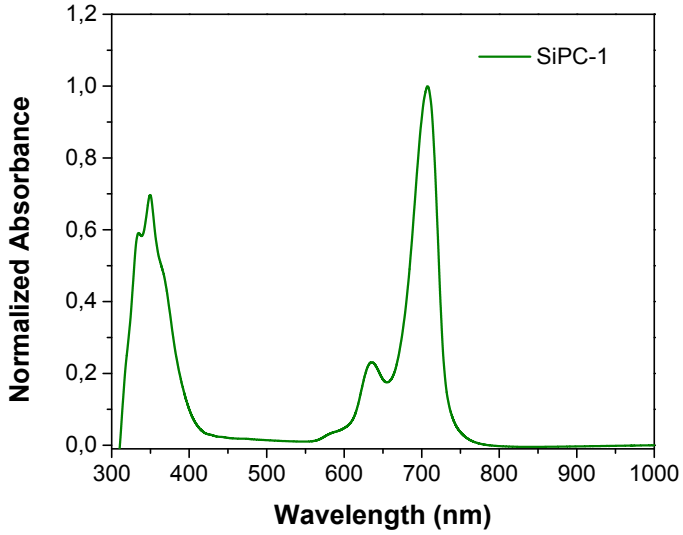

Fig. S9 Normalized absorption spectra of pristine **SiPC-1** in film.

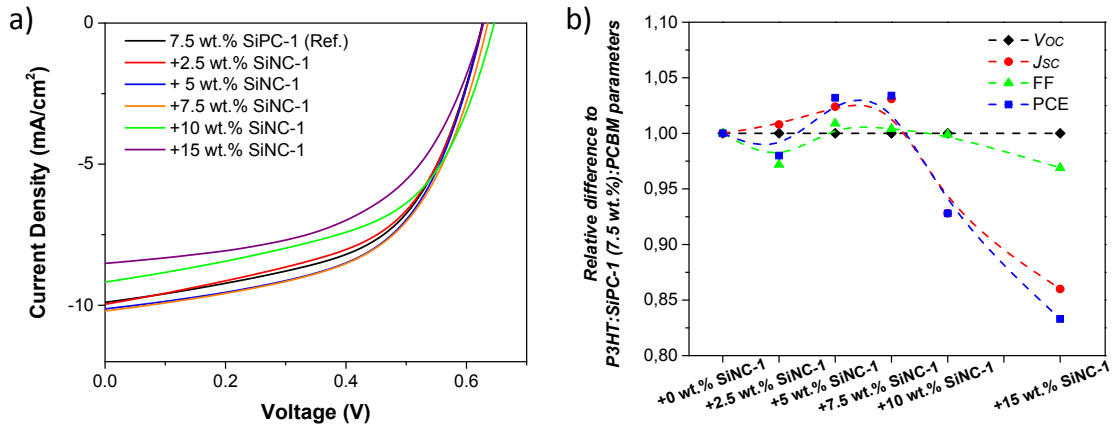

Fig. S10 a) *J–V* curves of P3HT:**SiPC-1**:**SiNC-1**:PCBM quaternary devices under different **SiNC-1** content; b) Relative changes of the device parameters with increasing **SiNC-1** content. The performance of ternary P3HT:**SiPC-1**:PCBM is chosen as reference and set to 100%. All other devices data are normalized to that reference.

Table S1 Photovoltaic device parameters of P3HT:**SiPC-1**:**SiNC-1**:PCBM ternary devices with 7.5 wt.% **SiPC-1** and different **SiNC-1** content under AM 1.5G, 100 mW cm^{-2}

Dye content	V_{OC}[V]	J_{SC}[mA cm^{-2}]	J_{SC}/EQE	FF[%]	Eff.[%]

SiPC-1[wt.%]+**SiNC-1**[wt.%]					
7.5%+0 %	0.65	9.89	8.29	54.15	3.48
7.5%+ 2.5%	0.65	9.97	8.36	52.65	3.41
7.5%+5%	0.65	10.13	8.51	54.63	3.59
7.5%+7.5%	0.65	10.20	8.71	54.35	3.60
7.5%+10%	0.65	9.18	8.32	54.08	3.23
7.5% +15%	0.65	8.51	7.75	52.47	2.90

[a]Note: the weight percent is referred to P3HT. The ratio of P3HT:PCBM is 2:1 for all devices. The values are averaged over 10 devices for each composition ratio.

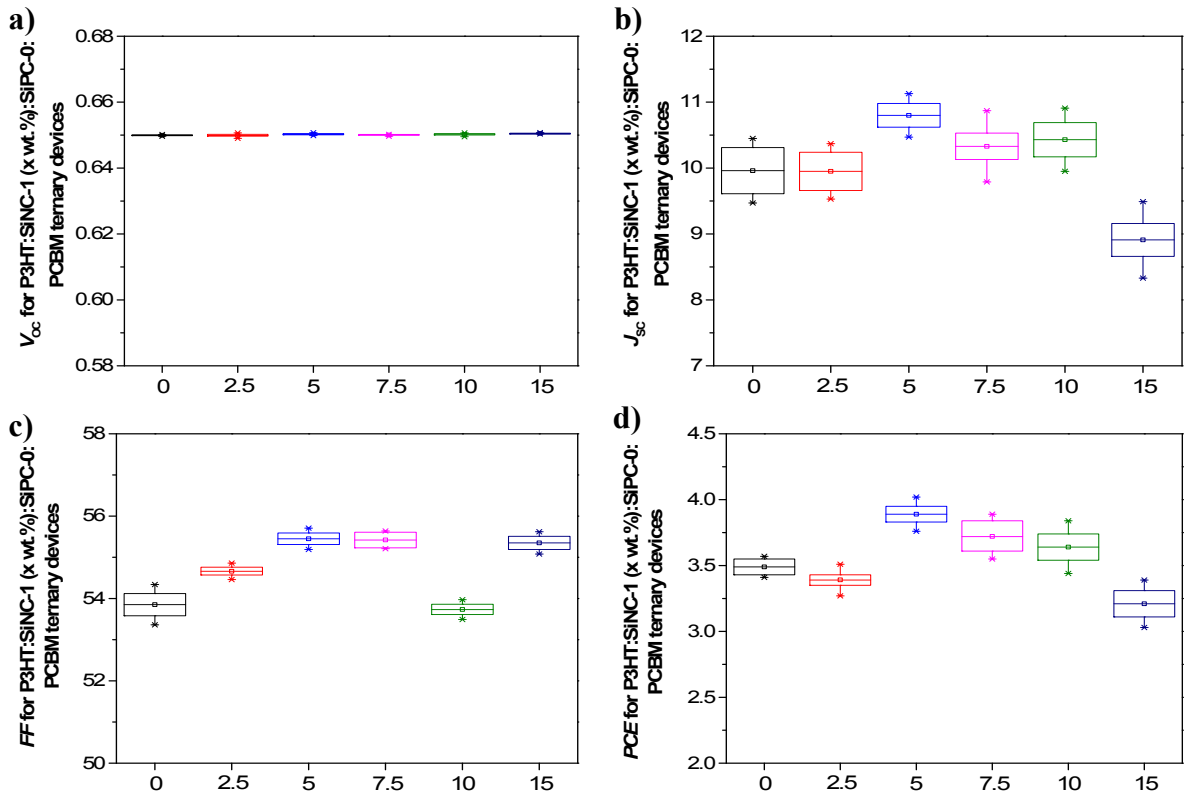

Fig. S11 Chart-box presentation of the a) V_{OC}, b) J_{SC}, c) FF and d) PCE values recorded for over 10 P3HT:**SiNC-1**:**SiPC-0**:PCBM quaternary blend solar cells versus **SiNC-1** contents. The concentration of **SiPC-0** is kept constant at 7.5 wt.%.

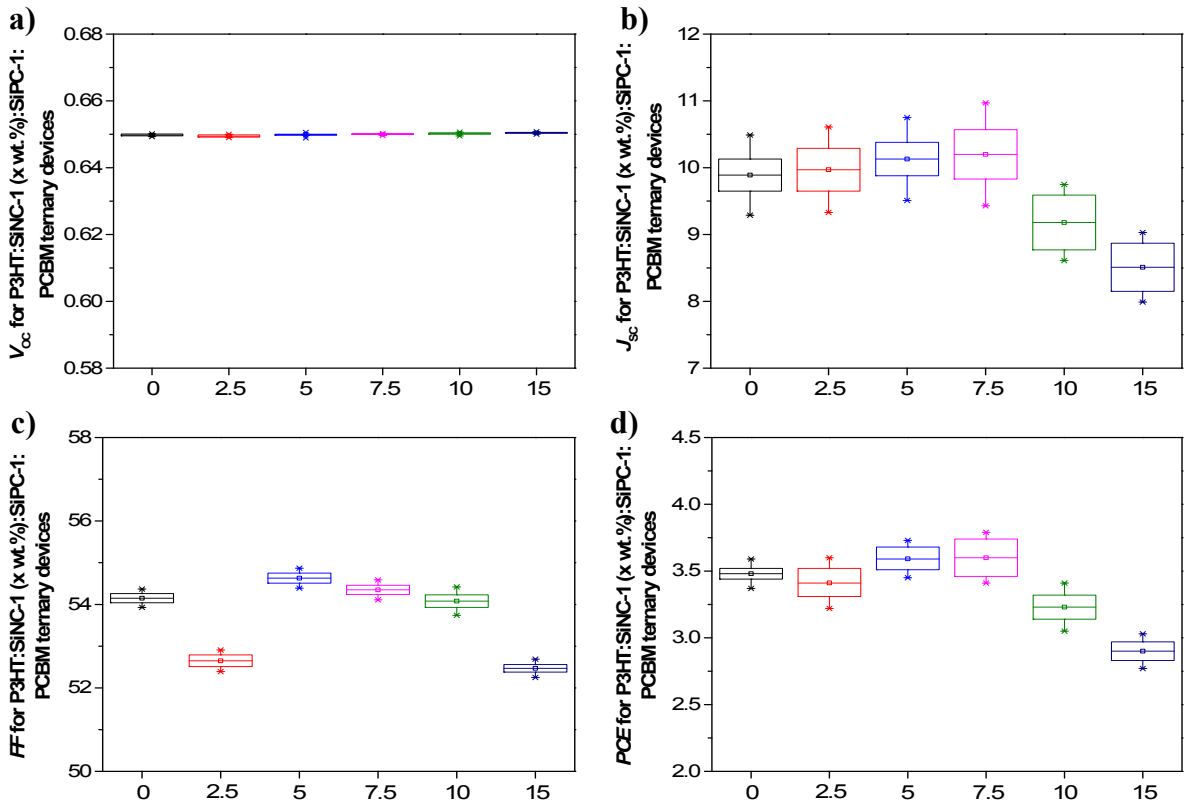

Fig. S12 Chart-box presentation of the a) V_{OC}, b) J_{SC}, c) FF and d) PCE values recorded for over 10 P3HT:**SiNC-1**:**SiPC-1**:PCBM quaternary blend solar cells versus **SiNC-1** contents. The concentration of the **SiPC-1** is kept constant at 7.5 wt.%.

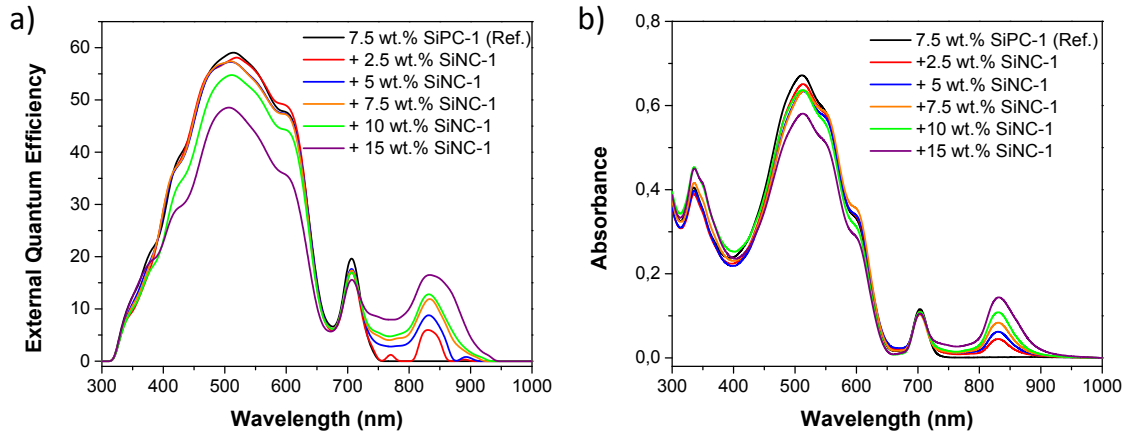

Fig. S13 a) EQE spectra of the P3HT:**SiPC-1**:**SiNC-1**:PCBM quaternary devices with increasing the **SiNC-1** content; b) Absorption spectra of the corresponding films.

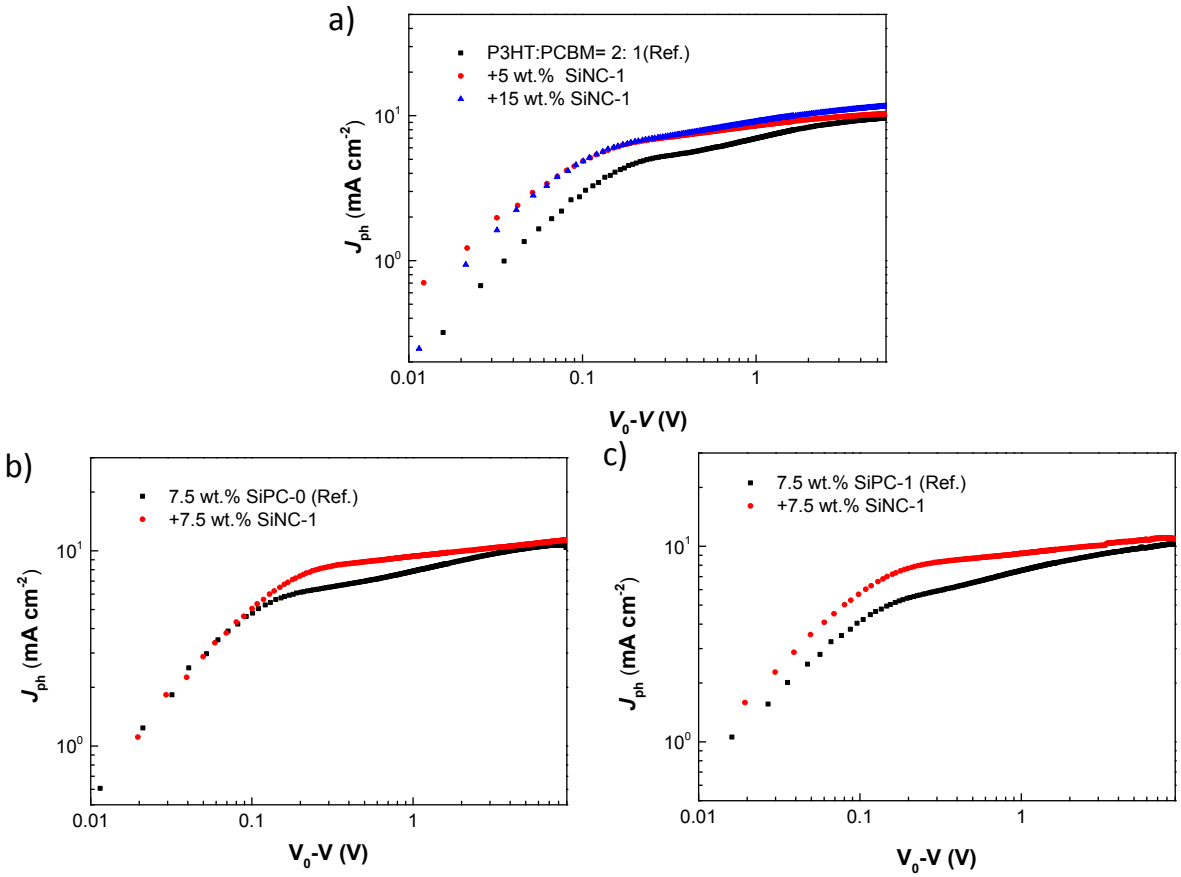

Fig. S14 Photocurrent density of a) P3HT: PCBM binary and P3HT:**SiNC-1**:PCBM ternary devices, b) P3HT:**SiPC-0**:PCBM ternary and P3HT:**SiPC-0**:**SiNC-1**:PCBM quaternary devices, and c) P3HT:**SiPC-1**:PCBM ternary and P3HT:**SiPC-1**:**SiNC-1**:PCBM quaternary devices as a function of the effective voltage under 1 sun illumination.

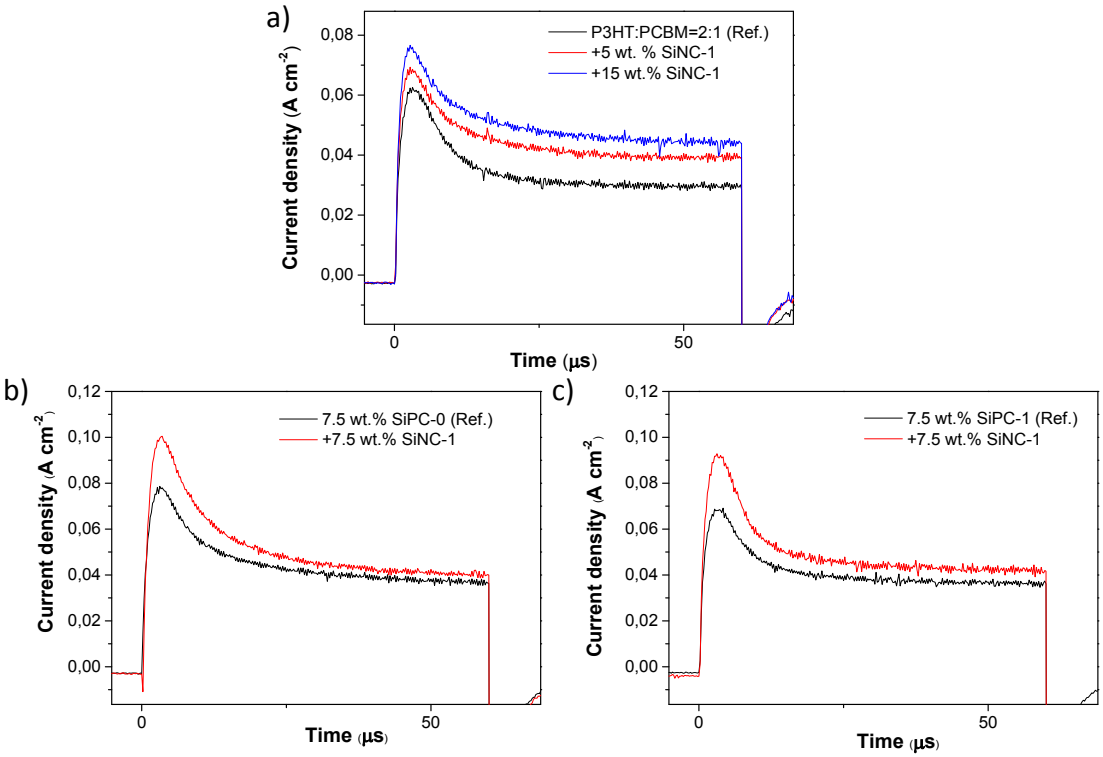

Fig. S15 Time-dependent photo-CELIV traces of a) P3HT:PCBM binary and P3HT:**SiNC-1**:PCBM ternary devices; b) P3HT:**SiPC-0**:PCBM ternary and P3HT:**SiPC-0**:**SiNC-1**:PCBM quaternary devices; c) P3HT:**SiPC-1**:PCBM ternary and P3HT:**SiPC-1**:**SiNC-1**:PCBM quaternary devices after a delay time of 50 µs.

Table S2 Summary of calculated charge carrier mobility (µ) by photo-CELIV for P3HT:PCBM binary, and **SiNC-1**, **SiPC-0**, **SiPC-1** based ternary and P3HT:**SiPC**:**SiNC-1**:PCBM quaternary devices.

Dye content	µ ($cm^2V^{-1}s^{-1}$)
P3HT:PCBM	$1.38x10^{-4}$
+5% **SiNC-1**	$1.49x10^{-4}$
+15% **SiNC-1**	$1.45x10^{-4}$
7.5% **SiPC-0**	$1.25x10^{-4}$
+7.5% **SiPC-0**+7.5% **SiNC-1**	$1.27x10^{-4}$
7.5% **SiPC-1**	$1.34x10^{-4}$
+7.5% **SiPC-1**+7.5% **SiNC-1**	$1.30x10^{-4}$

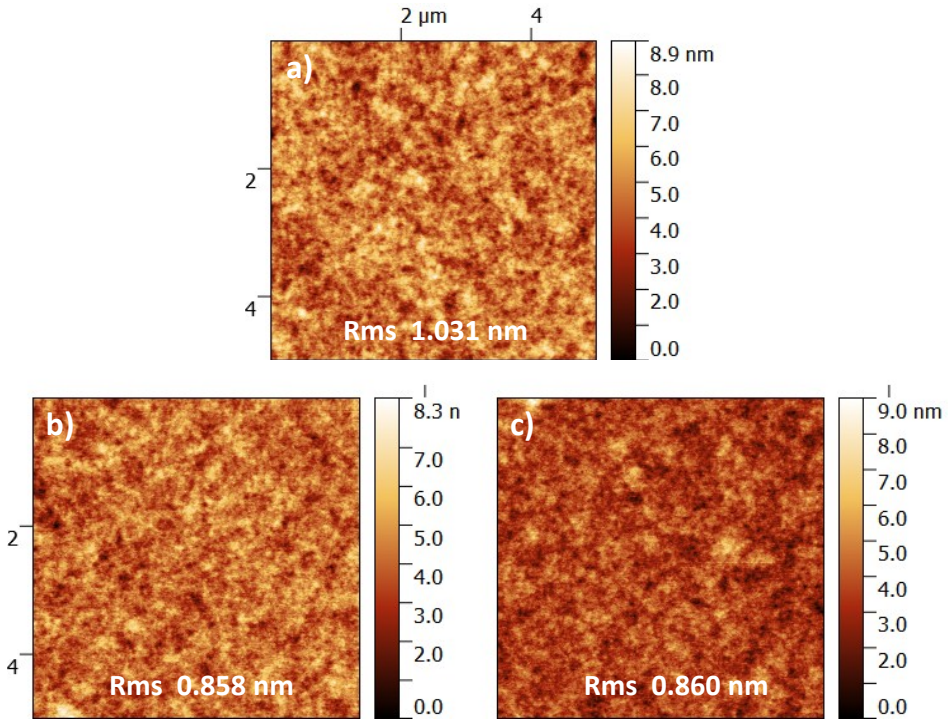

Fig. S16 Surface topographic AFM images (Size:10×10 µm^2) of a) binary P3HT:PCBM (2:1), b) ternary (15 wt.% **SiNC-1**), and c) quaternary (7.5 wt.% **SiNC-1**+7.5 wt.% **SiPC-0**) films.